# Search for Conical Intersection points (CI) by Newton Trajectories

Wolfgang Quapp,[1] Josep Maria Bofill[2] and Marc Caballero[3]

[1] *Mathematisches Institut, Universität Leipzig, PF 100920, D-04009 Leipzig, Germany*
*email: quapp@uni-leipzig.de Tel.: +49-341-97321-53 Fax: +49-341-97321-99*
*Web: http://www.mathematik.uni-leipzig.de/MI/∼quapp*
[2] *Departament de Química Orgànica, Universitat de Barcelona, c/Martí i Franqués, 1, 08028 Barcelona, Spain; and Institut de Química Teòrica i Computacional, Universitat de Barcelona (IQTCUB), c/Martí i Franquès, 1, 08028 Barcelona, Spain*
[3] *Departament de Química Física, Universitat de Barcelona, c/Martí i Franqués, 1, 08028 Barcelona, Spain; and Institut de Química Teòrica i Computacional, Universitat de Barcelona (IQTCUB), c/Martí i Franquès, 1, 08028 Barcelona, Spain*

**Abstract**

Recently, valley-ridge inflection points on the potential energy surface for the ring opening of the cyclopropyl radical have been determined using Newton trajectories (NT) [Quapp, Bofill, Aguilar-Mogas (2011) Theor Chem Acc 129:803]. This letter is the report about the utilization of NTs for the search for conical intersection (CI) points. These points play a main role in the understanding of intersections of different electronic surfaces which open the door for photochemical reactions. We explain the reason why Newton trajectories can find CI points, and report a CI seam on the CASSCF(3,3) surface of the allyl radical ring closure.

*Keywords:* Conical intersection point, Newton trajectory, Ring closure of allyl radical, Valley-ridge inflection point

## 1. Introduction: The Theory of Newton Trajectories and the Attraction of NTs by CI Points

The concept of the Potential Energy Surface (PES) is the basic ground of many theoretical chemistry models [1]. It is here an $n$-dimensional surface over the $n$ internal coordinates ($n = 3N - 6$) for an $N$-atomic molecule. Intersections of two or more electronic PES play a main role in the under-

standing of photochemical reactions. The key here is the event of a conical intersection (CI) [2, 3]. Up to date, the calculation of CI points is a difficult job which has to include all the involved electronic PESs for a constrained optimization, see references [4, 5, 6] and further references therein. From a general point of view, the methods to locate CI points can be classified according to the type of the objective function used for this task. Whereas in reference [4] the restrictions are imposed through a set of Lagrange multipliers, in the references [5] and [6] the restrictions are given implicitely by using the energy difference or its square form between the electronic states of the energy as objective function that are assumed to have at least a contact point.

Usually, CI points are not directly connected with the concepts of a Reaction Path (RP) and its more restrictive definition minimum energy path. On the ground state PES, the RP is defined as a continuous curve in the coordinate space, which connects two minimums of the PES by passing through a first order saddle point (SP), also called transition structure (TS). One special definition of an RP is the reduced gradient following (RGF) [7, 8, 9, 10, 11, 12, 13, 14] and its equivalent definition, the so-called Newton trajectory (NT) [15, 16]. In this letter, we extend the application of NTs to search a CI point on the ground state PES.

An NT can be calculated by an Euler-Branin-step method following along the direction of the vector field $\mathbf{Ag}$ of the so called Branin differential equation [17]

$$\frac{d\mathbf{x}(t)}{dt} = \pm\mathbf{A}(\mathbf{x}(t))\ \mathbf{g}(\mathbf{x}(t))\ , \tag{1}$$

where $\mathbf{A}$ is the adjoint matrix to the Hessian, its desingularized inverse, and $\mathbf{g}$ is the gradient of the PES. $t$ is a curve length parameter, $\mathbf{x}$ is the current point. A second definition of the NT is given by the projector equation

$$\mathbf{P_r g}(\mathbf{x}(t)) = \mathbf{0}\ . \tag{2}$$

The projector can be defined by a dyadic product with a normalized search direction, $\mathbf{r}$

$$\mathbf{P_r} = \mathbf{E} - \mathbf{r}\ \mathbf{r}^T\ , \tag{3}$$

where $\mathbf{E}$ is the unit matrix. Then the curve can be calculated numerically by the derivation of the projector equation along the curve parameter $t$ giving also the tangent of the NT [9]. The eq. (2) means that along an NT the

gradient always points into the **r**-direction.

Include Fig.1 near here!

Stationary points of the PES have a zero gradient. Thus, NTs into all directions can start from here if one adequately selects the sign of eq. (1) according to the index of the stationary point [8, 9, 18]. This means that the search direction of an NT, **r**, is optional from here. Thought inversely, this is the reason why stationary points are attractive points for NTs from all directions. An SP of index 2 on a PES is also the crossing point of infinitely many NTs, see Fig. 1. It is an attractor if we take the positive sign in eq. (1). There on the left hand side the summit surface -$x^2$-5 $y^2$ is shown, on the upper left hand panel, and on the lower line the field **Ag** is shown. The summit is at the point (0,0); it is an SP of index 2. Starting an NT uphill anywhere around the summit it will find the summit itself. Analogously, a funnel surface of a typical peaked $(n-2)$ CI event [2, 3] is shown on the right hand side of Fig. 1. It is the surface -sqrt($x^2$+5 $y^2$). Here, an analogous vector field **Ag** emerges. At this point it is important to emphasize that both types of problems, finding an SP of index two, a summit, or a peaked $(n-2)$ conical intersection point, are quite close, both conceptually and computationally. This is a hint that the NT method too finds CI points as well as summits. However, there are differences to the summit case:
**(i)** The two components of the gradient in the branching subspace do not go to zero around the peacked $(n-2)$-CI point, but hold any slope, and their direction is indefinite at the CI point. In Fig. 1 right panel the gradient is

$$\frac{1}{\sqrt{x^2+5y^2}}\,(x,5y)^T\ . \tag{4}$$

At $x=0$ and $y$ approximates zero, then the gradient points into the $y$-direction with value $\pm\sqrt{5}$, but at $y=0$ and $x$ approximates zero, then the gradient points into the $x$-direction with value $\pm 1$.
**(ii)** The two lowest Hessian's eigenvalues are indefinite values at the CI point because of the kink in the energy of any pathway passing the CI point. The Fig. 1 right panel is a simplified case. The two eigenvalues of the Hessian are

$$\left(0, -5\ (x^2+y^2)/\sqrt{x^2+5y^2}^{\,3}\right)\ . \tag{5}$$

The first eigenvalue belongs to the x-axis and concerns the points outside the apex; because the sign of the gradient direction jumps at the apex, the

eigenvalue here is indefinite as well. If the point $(x, y)$ moves to $(0, 0)$ then the second eigenvalue tends to minus infinity. In practical calculations, like the one reported here in this letter, the two lowest Hessian's eigenvalues are large negative values near putative CI points. (The Hessian is computed by finite differences.)
For the left summit case, on the other hand, the two negative eigenvalues describe the curvature transversally, as well as longitudinally to the summit. In a neighbourhood of the CI point, this may also hold for the PES around this point. But at the peak, the usual differential calculation breaks down. In a path calculation on the PES, we can follow an NT uphill to a CI point. The indicator to arrive at the CI region is the increase of the value $|\mathbf{Ag}|$ which itself becomes very large at the CI point. We find factors of $10^5$ and larger against "normal" NTs. The reason is the eigenvalues, $\mu_i$, of the $\mathbf{A}$ matrix, which go with the eigenvalues of the Hessian, the $\lambda_j$, j=1,...,n [18]

$$\mu_i = \prod_{j \neq i}^{n} \lambda_j \ . \tag{6}$$

The stopping criterium of the CI search, for the simple 2-dimensional case, would be a zigzagging of the predictor at the CI point. This can be indicated. In the high-dimensional praxis on the CASSCF surface, indefinite eigenvalues of the Hessian do not emerge. The quick increase of the $|\mathbf{Ag}|$ value is a first sign that the NT is attracted by a CI point. Then anywhere happens a saturation. The CI seam is reached. Of course, a second indicator is a bad convergence of the CASSCF calculation. (We stop the calculation by hand.)
**(iii)** For an SP of any index, the gradient has to be zero. Thus, the SP is an NT-attractor in all dimensions if we take the appropriate sign in eq. (1). The CI kink concerns a two-dimensional subspace of the configuration space. For higher dimensional problems it is recommended first to estimate the two vectors, $\mathbf{vd}, \mathbf{vc}$, that define the linear subspace called branching subspace, $S_b$, and its orthogonal complement called the tangent intersection subspace, $S_{ti}$ [4]. The two basis vectors of the $S_b$ subspace are the difference vector, $\mathbf{vd}$, and the coupling vector, $\mathbf{vc}$,

$$\mathbf{vd} = \nabla_{\mathbf{x}}(\mathbf{W}_{1,1}(\mathbf{x}) - \mathbf{W}_{2,2}(\mathbf{x})) \tag{7}$$

$$\mathbf{vc} = \nabla_{\mathbf{x}}(\mathbf{W}_{1,2}(\mathbf{x})) \tag{8}$$

where $\mathbf{W}_{i,j}(\mathbf{x})$ is the $ij$ element of the matrix $\mathbf{L}(\mathbf{x})$ of the corresponding Lagrange problem [4]. The set of vectors that defines the basis of the $S_{ti}$

subspace is taken orthogonally to the **vd** and **vc** vectors [4]. If the latter two vectors are collected in a rectangular matrix, $\mathbf{T}_b = [\mathbf{vd}\,\mathbf{vc}]$, and if the set of vectors of the $S_{ti}$ subspace is collected in a $\mathbf{T}_{ti}$ submatrix, then both rectangular submatrices build the transformation matrix, $\mathbf{T} = [\mathbf{T}_b\mathbf{T}_{ti}]$ which transforms the given $\mathbf{x}$ coordinates into new ones. Notice that $\mathbf{T}$ itself depends on the $\mathbf{x}$ coordinates. The process is summarized through the transformation [4],

$$\Delta\mathbf{q} = [\mathbf{T}_b\mathbf{T}_{ti}]^T\Delta\mathbf{x}\ . \tag{9}$$

One could apply the NT method in the new coordinate space. However, following NTs which lead to a CI point on the seam, automatically also lead to vectors in the subspace $\mathbf{T}_b$. Because these are two negative eigenvalues of the original Hessian of the ground state at, or near the crossed CI point. The mathematical proof of the statement is based on Löwdin's partitioning technique [19] and will be outlined in a next paper.

A technical problem is the following: Near CI points the Newton-Raphson method for corrector steps often fails, if we use the derivation of eq.(2). Then we only work with predictor steps along eq.(1), and we omit the corrector steps. The resulting NT is named quasi-NT, because it can deviate a little from the true one, especially if it is strongly curved. Such predictor-only steps work properly, because the $\mathbf{A}$ matrix is the desingularized inverse of the $\mathbf{H}$ matrix. It is calculable if the $\mathbf{H}$ matrix is given.

Configuration interactions can take place in a sloped kind [2, 3]. Such events are not found by the funnel search which we report here, because they do not show the pattern of the $\mathbf{A}\,\mathbf{g}$ vector field which we need here. However, a quasi-NT search can also do well for sloped CI seams. If a seam is crossed then the vector $\mathbf{A}\,\mathbf{g}$ usually jumps to another direction. The corresponding quasi-NT will show a sharp kink. We can study such nodes and do a corresponding control calculation for upper surfaces. Examples can be found in Figs. 8,9,11 and 12 of reference [20].

## 2. Attraction of quasi-NTs by CI points on the PES of the allyl radical ring closure

In Organic Chemistry the prediction of stereochemistry of the electrocyclic ring closure reactions has been a long-standing question. For cyclic

molecular structures in their ground state with an even number of electrons the reactions are governed by the Woodward-Hofmann rules [21]. The rules either predict a conrotatory or disrotatory stereochemistry evolution depending on the orbital diagram associated to the system. For the cyclopropyl radical, a system with an odd number of electrons, the Woodward-Hofmann rules predict that both the conrotatory and disrotatory stereochemistry evolution are nominally forbidden [22]. In the study [22] a highly asynchronous transition structure with $C_1$ symmetry was identified. In a later study at the B3LYP/6-311G(2d) level of theory [23], the calculation of the intrinsic reaction coordinate was carried out from the $C_1$-TS to the allyl radical. The unsymmetric pathway avoids the crossing of CI points which are expected on the PES [24].

For the purpose of this letter, our consideration of the allyl radical is purely a test system for a search of CI points. Fig. 2 shows the atom labels of the allyl radical that will be used. The GAMESS-US program is utilized for the quantum chemical calculations by the CASSCF(3,3)/6-31G(d,p) method [25]. The NT-programs (in Fortran) can be downloaded from the web-page www.math.uni-leipzig.de/∼quapp/SkewVRIs.html. Any tracing along NTs uses the curvilinear internal coordinates in the full dimension of $n = 3N-6 = 18$. At every node of an NT, the metric matrix is taken from the GAMESS-US program to convert co- and contra-variate objects, as well as the energy, the gradient and the Hessian of the lowest electronic PES. In the z-matrix, the distances are given in Å, and the angles and the dihedrals are given in degrees, where in the GAMESS-US part Bohr and radiant units are used.

```
z-matrix        allyl radical
C1
c1
c2  1  r1
c3  1  r2   2  c2c1c3
h4  1  hc1  2  hcc1   3  dih1
h5  2  hc2  1  hcc2   3  dih2
h6  3  hc3  1  hcc3   2  dih3
h7  2  hc4  1  hcc4   3  dih4
h8  3  hc5  1  hcc5   2  dih5
```

Include Fig. 2 near here!

In the foregoing papers [20, 26, 27], we confirmed a valley-ridge inflection (VRI) point at the allyl radical end of the SP col. It was named $VRI_{ca}$ to characterize the direction from the cyclopropyl bowl, the symbol is the lower case letter $c$, over $SP_{ca}$ into the allyl radical bowl, the symbol is the lower case letter $a$. NTs are the curves which are well adapted to search for VRIs because they bifurcate there. The method of the search of VRI points is described in ref. [28].

A VRI system of a bifurcating, singular NT consists of four branches. The character of the single branches determines the character of the VRI point. All VRI points can be classified into different main classes. A valley starting from an SP can bifurcate downhill and the two branches can lead to two valleys with their corresponding minimums. Between the two valleys a ridge emerges. However, the $VRI_{ca}$ does not have this character. There is another possibility that a ridge on the PES bifurcates into two ridges, and between the two ridges emerges a valley. Then the VRI point is a ridge-pitchfork (rpVRI) bifurcation. The $VRI_{ca}$ is of this character. The corresponding ridge from below is guessed to come from one of the allyl SPs, named $SP_{aa}$. They have a turned methylene group at one end, where the other methylene remains in the plane of the C-atoms [20, 27]. If the methylene 1 group is turned out off the C-plane then the SP gets the index (2,4) where in the contrary case, if the methylene 2 group is turned, the index will be (3,5). Additionally to the $VRI_{ca}$, we found VRI points near the SPs in the allyl radical bowl, the $SP_{aa}$. These new VRIs are on the ridge over the $SP_{aa}$. The are named $VRI_{ac}$ to accentuate their local connection to the allyl bowl. The character of the points found is either rpVRI or of the mixed type where ridges of a different index cross [20].

Include Fig. 3 near here!

Using the PES of the very floppy allyl radical as an example, we tried to make relaxed surface scans of diverse dihedrals to generate a 2D surface. But we were not successful to create the usual, meaningful level lines in 2D subspaces of the configuration space in the past. There are too many dimensions where the PES changes. However, NTs are curves in the full-dimensional configuration space. They characterize a skeleton of valley- and ridge-lines. Their projection into 2-dimensional planes can be used to generate an imagination of the full PES. This is done in Fig. 3. We report a new

**Table 1** Coordinates of $VRI_{low}$, of $VRI_{up}$, and an adjacent CI point in the order of the z-matrix (with energy in hartree, $E_h$)

| $VRI_{low}$ (-116.450 957) | | | $VRI_{up}$ (-116.311 746) | | | CI (-116.333 590) | | |
|---|---|---|---|---|---|---|---|---|
| 1.490 | | | 1.528 | | | 1.486 | | |
| 1.360 | 113.42 | | 1.413 | 97.11 | | 1.492 | 97.78 | |
| 1.097 | 98.89 | -153.11 | 1.214 | 71.52 | -142.63 | 1.113 | 96.84 | -136.00 |
| 1.081 | 114.66 | 82.02 | 1.087 | 108.32 | 71.24 | 1.082 | 112.59 | 58.68 |
| 1.083 | 118.73 | 17.00 | 1.093 | 117.25 | 31.86 | 1.085 | 113.23 | 56.29 |
| 1.077 | 124.12 | -124.46 | 1.083 | 127.45 | -149.10 | 1.079 | 126.57 | -150.24 |
| 1.057 | 123.63 | -158.97 | 1.043 | 127.57 | -131.27 | 1.081 | 113.48 | -73.34 |

VRI point of the character $ac\_2, 4$, compare ref. [20] which is here depicted by $VRI_{low}$. Its side branches lead to CI points where the central branch exhausts a valley. A further VRI point, $VRI_{up}$, is found upwards in the PES region, which is connected with $VRI_{low}$ over the central branch. Its central branch then leads uphill to the CI seam.

The representation is the following. We use the projection of one and the same full-dimensional quasi-NT to the both dihedrals, dih2 or -dih5, and the ring closure angle, in the left panel, as well as to the dih3 or -dih4, and the ring angle in the right panel. So, every panel contains two pictures of the singular quasi-NT of interest. The abscissae is the "reaction coordinate". It is the angle between the C-atoms, compare Fig. 2, which describes the ring closure of the allyl radical, from the right hand side to the left hand side. The singular quasi-NT is a fat curve. In both panels further bullets are included for dihedrals of the following special points: $VRI_{low}$, $VRI_{up}$ (see Table 1) and the points $SP_{aa}$, $SP_{ca}$, and $VRI_{ca}$ (see ref. [20]). (For the latter all four bullets are included in every panel.) Their values on the abscissae are also highlighted by grid lines. All bullets on one upright grid line belong to one of the special points. Their descriptions emerge once on the grid line. The order of the bullets for $SP_{ca}$ and $VRI_{ca}$ is, from top to bottom, dih2, -dih5, dih3 and -dih4. Note, that the order of the bullets for the special points on the right hand side is another.

The new VRI points, $VRI_{low}$ and $VRI_{up}$, of Fig. 3 (see coordinates in Table 1) are a very special case where the two outer branches of the lower

bifurcating quasi-NT were attracted, after the bifurcation and after a long way over the PES, nearby by a CI seam. The central branch of the upper VRI also leads to this CI seam. Usually, the three branches of a singular NT wander after the bifurcation into different regions of the PES; that is even the character of a bifurcation to create dividing valleys or ridges.

The character of the lower $\mathrm{VRI}_{low}$ point is rpVRI, a ridge pitchfork. The ridge of index one from $\mathrm{SP}_{aa\_2,4}$ bifurcates into two outer forks being also ridges of index one, and into one central branch being a valley line. All three branches climb uphill on the energy surface, however the quasi-NTs of the outer branches later meet the seam at CI points symbolized by a '*'. One branch touches the seam and is then "reflected", thus goes again downhill to the $\mathrm{SP}_{aa}$ region (the reflected part is not shown in Fig. 3). The other branch touches the seam and scans then along the seam. The scan-part is built by the bold nodes in Fig. 3, which are somewhat not smooth. After a long piece gliding along the seam, it also turns downhill to the $\mathrm{SP}_{aa}$, by a turn near $106^o$ of the ring angle. A putative CI point is given in Table 1.

The quasi-NT of the central branch of $\mathrm{VRI}_{low}$ starts as a valley line uphill. Then it forms a repeated circular pathway being more or less inside the outer branches. At the end of the valley, it meets the second VRI point, $\mathrm{VRI}_{up}$. The character of the upper $\mathrm{VRI}_{up}$ point is also of rpVRI. The central branch comes uphill as a valley and goes further uphill to the CI seam as a ridge. If one uses the plus sign in Eq.(1) for the funnel search then the calculation scans along a seam going uphill in energy. (A minus sign would repel nodes from the summit.) Thus in this case the quasi-NT scan goes off from the usually searched minimum energy conical intersection. In the case of the seam in Fig. 3 we use the other method: we go along $\mathbf{A}\,\mathbf{g}$ direction in eq.(1) but always use the sign "forward", into the same "halfspace". It is the usual strategy to follow a quasi-NT. The $\pm$ sign can then be used to decide to go uphill or downhill on the PES. Using this and sliding along the seam, the method glides a little along the seam, but then it jumps over the seam and goes down the other side to the $\mathrm{SP}_{ca}$. (The piece of the NT is not shown in the picture.) One side branch from the upper $\mathrm{VRI}_{up}$ also returns as a ridge line into the valley region as a circular curve. After some circles over as well as below the central branch, it breaks out and goes down to $\mathrm{SP}_{aa}$. The other side branch turns up as a ridge and goes directly anywhere into the PES mountains (not shown further).

We try to explain first the behaviour of the outer branches of $\mathrm{VRI}_{low}$, as well as the central branch of $\mathrm{VRI}_{up}$: they suffer under a quick increase of the $|\mathbf{Ag}|$ value. The two first eigenvalues of the Hessian from an output of GamessUS at the crossing of the central branch with the seam are: $\lambda_1 = -1.75$, $\lambda_2 = -0.051$, so to say, that are moderate values. In the middle of the seam, there is a point with $\lambda_1 = -34.44$, $\lambda_2 = -2.16$ in the internal coordinates of GamessUS: in Bohr and radiant units. The absolute values are considerably large values. Usual eigenvalues in these units are $\approx \pm\, 0.1$. A bizarre observation is that also the largest eigenvalue on the seam is very large: $\lambda_{18} = 11.44$ . We do not have an explanation for this number. The corresponding values for the CI point of Table 1 are: $\lambda_1 = -24.40$, $\lambda_2 = -3.182$ and $\lambda_{18} = 6.956$, where the minimum energy point at the end of the seam has: $\lambda_1 = -14.61$, $\lambda_2 = -3.77$ and $\lambda_{18} = 3.55$ .

The connection, using $\mathrm{VRI}_{low}$ as a knot, of the SP of index one, $\mathrm{SP}_{aa}$, and a CI point playing the role of a summit, an SP of index two, by the outer branches of the quasi-NT of $\mathrm{VRI}_{low}$ shows an index difference by one. It does not violate the index theorem for NTs [29, 30] that a regular NT (without a VRI point) cannot connect two stationary points of the same index.

We guess that the CI points of the seam have a peaked topology [31], because we find two negative eigenvalues of the Hessian there. A further hint for a peaked topology is the following: different steepest descent pathways from the putative CI points go into accidental directions. It is a hint that such a point is like a summit. For a sloped CI, the direction would be fixed. The found CI points are not symmetric in the dihedrals. However, the distances $r1$ and $r2$ cross near some CI points their symmetry line at $r1 = r2 = 1.492\,8$. One should compare other symmetric CIs found in refs.[32, 33].

We guess that the growing string of the special branches of the singular quasi-NT meet the CI seam (by accident) anywhere and then we can jump over it, or we can scan along the CI seam with the quasi-NT. The condition for meeting the seam at all is that the search direction of the current quasi-NT fulfills the equation

$$1/Norm * ([\mathbf{vc}\,\mathbf{vc}^T + \mathbf{vd}\,\mathbf{vd}^T]\mathbf{g}) = \mathbf{r}\ , \tag{10}$$

being $\mathbf{r}$ the selected direction by the actual NT with eq. (1). $1/Norm$ is a

normalization constant, and **vc**, **vd** are the vectors of the branching $\mathbf{T_b}$ subspace, see eqs. (7) and (8). Using the "forward" strategy along the seam by a search direction with formula (10), we can descend to a putative minimum energy point on the conical intersection seam at $106^o$ of the ring angle, see Fig. 3. The energy difference of the first seam crossing point of the three branches of the singular quasi-NT, and the minimal node, is from -116.28 $E_h$ to -116.37 $E_h$, see Fig. 4. At all, one should keep in mind that a quasi-NT slips from one true NT to another, step by step, and it can therefore end up at a different search direction than the NT it started from (though our predictor step length is very small). Figure 3 suggests that the branch connecting $\mathrm{VRI}_{up}$ with $\mathrm{SP}_{aa}$ does not belong to the same NT as the branch that connects $\mathrm{SP}_{aa}$ and $\mathrm{VRI}_{low}$. However it emerges to a miracle that the central branch connects the $\mathrm{VRI}_{low}$ with the $\mathrm{VRI}_{up}$.

Include Fig. 4 near here!

A control calculation at a putative CI point of the seam, see Table 1, was done. A CASCI calculation of the corresponding first excited electronic surface, $\tilde{A}^2B$, at this configuration confirms the conjecture to be at a CI point: It is based on the natural orbitals extracted from the CAS(3,3) (quartet) set. The energy difference between the two doublet states is 0.5 kcal/mol, it is an excellent value. The description of the three states is
state 1: energy=-116.328 448 481, S=0.5,
state 2: energy=-116.327 647 388, S=0.5,
state 3: energy=-116.315 182 186, S=1.5,
and SZ=0.5, space sym=A holds in all three cases.

Include Fig. 5 near here!

The central branch of the lower VRI point, $\mathrm{VRI}_{low}$, needs a second explanation, as well as the existence of the upper $\mathrm{VRI}_{up}$ crossed by one singular NT. The lower central branch circulates five and a half times around a valley of the PES, up to the upper VRI point. The circular curves implicate the possibility that an NT can be quite convoluted on a hilly PES. In each case the uphill pathway is a valley line going up to a turning point, where the quasi-NT turns and goes parallel downhill. Then this pathway is a ridge line going down back to the initial region. And so on, five and a half rounds up to $\mathrm{VRI}_{up}$.

There is a simplified analogy to a circular NT on a simple 2-dimensional surface, see the right panel of Fig. 5 which may be compared with Fig. 3.11 of ref. [30], the so-called dent of a thumb. Maybe that the example can explain the behaviour of the circular pieces of the NT in Fig. 3. The formula of a 2-dimensional toy surface on the left hand side is

$$sl(x,y) = x^2\,(x^2 - 2 + 1.5\,y) + y^2\,(y-4)^2 - 25\,\sqrt{x^2 + 3\,(y-2)^2} \qquad (11)$$

and additionally, for the right panel a dent is pressed into the ridge on the y-axis:

$$sr(x,y) = sl(x,y) - 25\,exp(-3.48\,x^2 - 4\,(y-1.093)^2)\ . \qquad (12)$$

The level lines of the PES are thin lines, where families of NTs are represented by bolder lines. In the left panel, a "usual" surface is drawn. Here two singular NTs of the mixed type connect the two lower minimums with the CI point at the top crossing one of the VRI points, and the other branches connect different SPs. On the right panel, an additional dent is pressed into the ridge which leads from the lower SP to the CI point. Now the VRIs are moved a little, and new compact NTs emerge. The dent on the slope of the ridge surface is filled by a pair of families of compact NTs, and a new singular NT (the dashes on the y-axis) divides the families. The singular NT crosses a lower VRI point at ≈(0.0,0.2), and a further, upper VRI point at ≈(0.0,1.7). Both VRIs are rpVRIs. The inner, circular NTs inside the dashed, singular NT do not cross stationary points or VRIs. They are compact curves. Note, the molecular case on the PES in Fig. 3 may be a little more complicated. There are 18 dimensions for the PES. The central branch of the singular NT is a spiral line which cannot be in a 2-dimensional plane. Note further that the CI points first found must not be a minimum, or an SP on the high-dimensional seam, compare the refs.[31, 34].

## Conclusion

Up to date, the calculation of CI points is a difficult job, see references [4, 5, 6] and further references therein. We have "simply" used the numerical following along quasi-NTs on the ground adiabatic PES and this leads to peaked CI points quite in analogy to the finding of SPs of index 2 [8, 9]. The coordinates of a pututive CI point on the allyl radical PES are given

in Table 1. We think that we did not find the exact CI, however the point is assumed to be near the apex of the corresponding conoid. In Fig. 3 we depict the projection of quasi-NTs into 2-dimensional planes. Even though quasi-NTs are curves in the full-dimensional configuration space, we assume that we can use their projections for four different, but important dihedrals to generate an imagination of the PES. NTs characterize a skeleton of valley- and ridge-lines. They bifurcate where valleys or ridges of the PES bifurcate. In the case discussed here, we find that a long valley exists on the ridge on the allyl radical PES (without an intermediate minimum), if one leaves the $SP_{aa}$ uphill in a corresponding ridge direction. The lower entrance into the valley goes through a VRI point. The upper departure gate is also a VRI point like in Fig. 5. On the high-dimensional PES, the pathway of the central branch leaves the valley and later crosses the CI seam, as well as the two lower side branches. At the top near the former valley, a long CI seam is placed. The new avenue to find the structures is the Newton trajectory method.

Acknowledgments
Financial support from the Spanish Ministerio de Economía y Competitividad, DGI project CTQ2011-22505 and, in part from the Generalitat de Catalunya projects 2009SGR-1472 is fully acknowledged. M.C. gratefully thanks the Ministerio de Economía y Competitividad for a predoctoral fellowship.
We thank two referees for many helpful suggestions and comments.

## References

[1] D. Heidrich (Ed), The Reaction Path in Chemistry: Current Approaches and Perspectives, Kluwer, Dordrecht, 1995.

[2] D.R. Yarkony, Rev Mod Phys 68 (1996) 985.

[3] M.J. Bearpark, M.A. Robb, H.B. Schlegel, Chem Phys Lett 223 (1994) 269.

[4] J.M. Anglada, J.M. Bofill, J Computat Chem 18 (1996) 992.

[5] F. Sicilia, L. Blancafort, M.J. Bearpark, M.A. Robb, J Theor Chem Computat 4 (2008) 257.

[6] S. Maeda, K. Ohno, K. Morokuma, J Chem Theo Computat 6 (2010) 1538.

[7] I.H. Williams, G.M. Maggiora, J Mol Struct (Theochem) 89 (1982) 365.

[8] W. Quapp, M. Hirsch, D. Heidrich, Theor Chem Acc 100 (1998) 285.

[9] W. Quapp, M. Hirsch, O. Imig, D. Heidrich, J Comput Chem 19 (1998) 1087.

[10] W. Quapp, J Comput Chem 22 (2001) 537.

[11] M. Hirsch, W. Quapp, J Comput Chem 23 (2002) 887.

[12] J.M. Anglada, E. Besalu, J.M. Bofill, R. Crehuet, J Comput Chem 22 (2001) 387.

[13] J.M. Bofill, J.M. Anglada, Theor Chem Acc 105 (2001) 463.

[14] R. Crehuet, J.M. Bofill, J.M. Anglada, Theor Chem Acc 107 (2002) 130.

[15] W. Quapp, J Molec Struct 695-696 (2004) 95.

[16] J.M. Bofill, W. Quapp, J Chem Phys 134 (2011) 074101.

[17] F.H. Branin, IBM J Res Develop 16 (1972) 504.

[18] M. Hirsch, W. Quapp, J Math Chem 36 (2004) 307.

[19] P.-O. Löwdin, in: Perturbation Theory and Its Application in Quantum Mechanics, C. H. Wilcox (Ed) Wiley, New York, 1966, p. 255.

[20] W. Quapp, J.M. Bofill, J Math Chem *in print* (2012)
DOI 10.1007/s10910-012-9995-8.

[21] R.B. Woodward, R. Hoffmann, J Am Chem Soc 87 (1965) 395.

[22] S. Olivella, A.Solé, J.M. Bofill, J Am Chem Soc 112 (1990) 2160.

[23] P.A. Arnold, B.K. Carpender, Chem Phys Lett 328 (2000) 90.

[24] Y. Haas, S. Cogan, S. Zilberg, Int J Quant Chem 102 (2005) 961.

[25] Gamess-US program: M.V. Schmidt, et al., J Comput Chem 14 (1993) 1347.

[26] A. Aguilar-Mogas, X. Giménez, J.M. Bofill, J Comput Chem 31 (2010) 2510.

[27] W. Quapp, J.M. Bofill, A. Aguilar-Mogas, Theoret Chem Acc 129 (2011) 803.

[28] W. Quapp, B. Schmidt, Theor Chem Acc 128 (2011) 47.

[29] I. Diener, Globale Aspekte des kontinuierlichen Newtonverfahrens, Habilitation, Universität Göttingen, Germany, 1991.

[30] M. Hirsch, Dissertation (Ph.D.Thesis), Universität Leipzig, Germany, 2004.

[31] G.J. Atchity, S.S. Xanteas, K. Ruedenberg, J Chem Phys 95 (1991) 1862.

[32] L. Castiglioni, A. Bach, Phys Chem Chem Phys 8 (2006) 2591.

[33] M. Shahu, Int J Quant Chem 106 (2006) 501.

[34] F. Sicilia, L. Blancafort, M.J. Bearpark, M.A. Robb, J Phys Chem A 111 (2007) 2182.

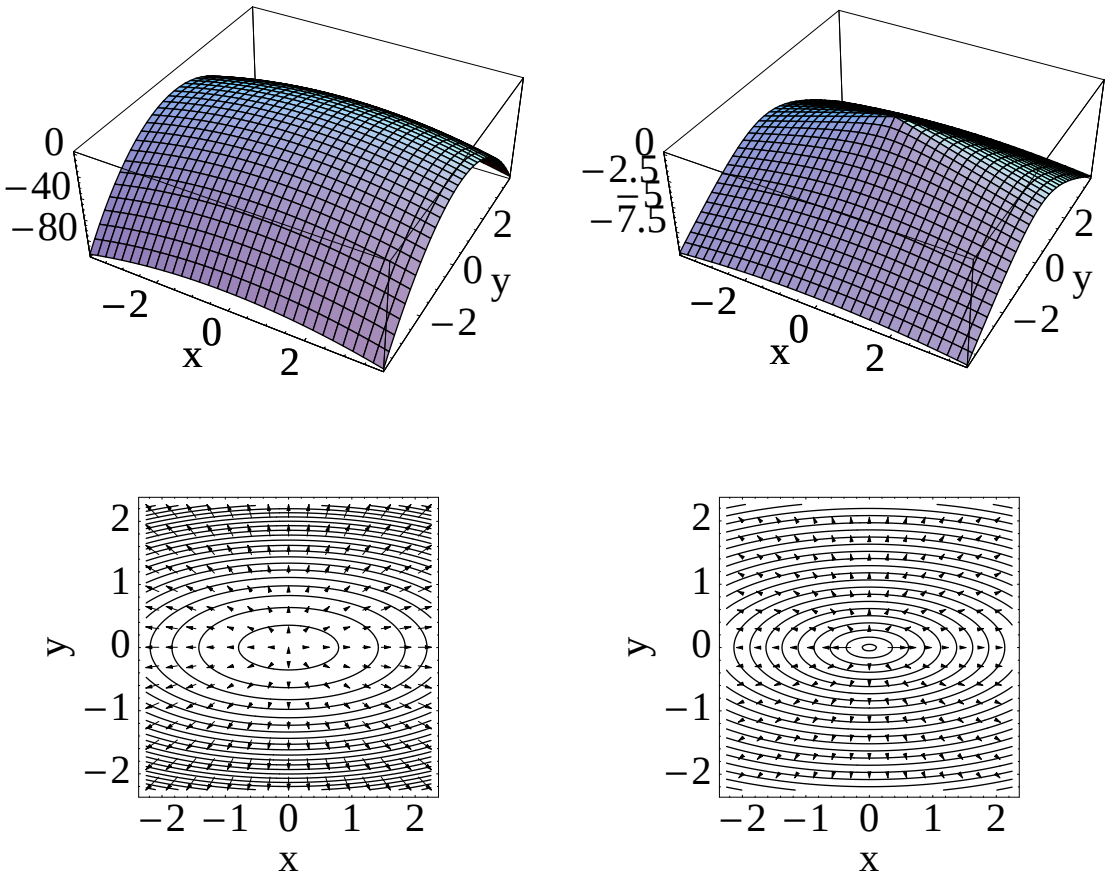


Figure 1: Summit surface on the left hand side, and funnel on the right: both have analogous **Ag** fields shown below.

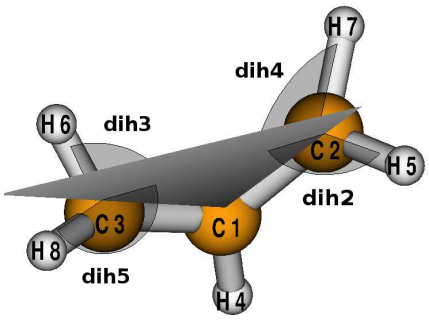


Figure 2: Ring closure of the allyl radical: numbering of atoms in the z-matrix

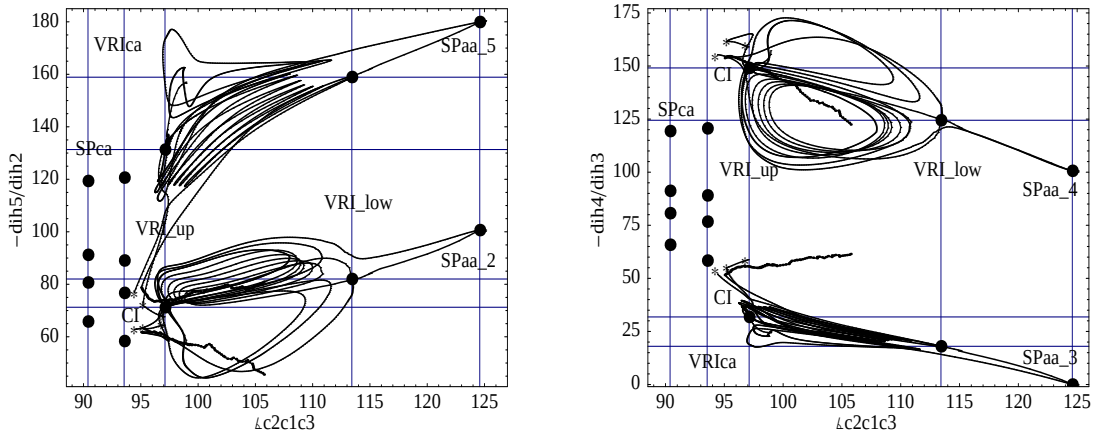


Figure 3: Singular NT in the region over the transition state, $SP_{aa}$, along a ring closure of the allyl radical. The PES construction is based on the functional energy CASSCF(3,3)/6-31G(d,p). Bullets with a cross of grid lines are the VRI points, $VRI_{low}$ and $VRI_{up}$, see text. The $*$ symbols indicate the CI seam reached by different branches of the singular quasi-NT. The bold, but not smooth curve is a part of the seam, scanned by one quasi-NT. **Left**: coordinates are the angle between the C-atoms, and the two dihedrals dih2 and -dih5. **Right**: the same quasi-NT for the ring-angle and the two dihedrals dih3 and -dih4. (For comparison the old known $VRI_{ca}$ point is added. It is at the end of the $SP_{ca}$ col, see ref. [20].)

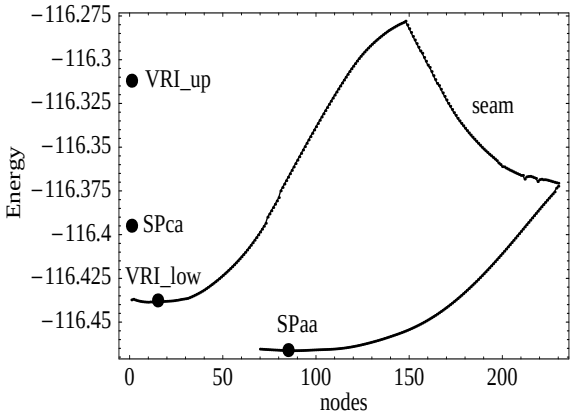


Figure 4: Energy profile along an outer branch of the singular quasi-NT in $\mathrm{VRI}_{low}$, along a ring closure of the allyl radical, up to the CI seam, then gliding downhill along the seam, and then going downhill back to $\mathrm{SP}_{aa}$. (The last piece of the quasi-NT is not shown in Fig. 3.) Bullets depict the energy of special points, like $\mathrm{VRI}_{low}$, $\mathrm{VRI}_{up}$, $\mathrm{SP}_{ca}$ and $\mathrm{SP}_{aa}$.

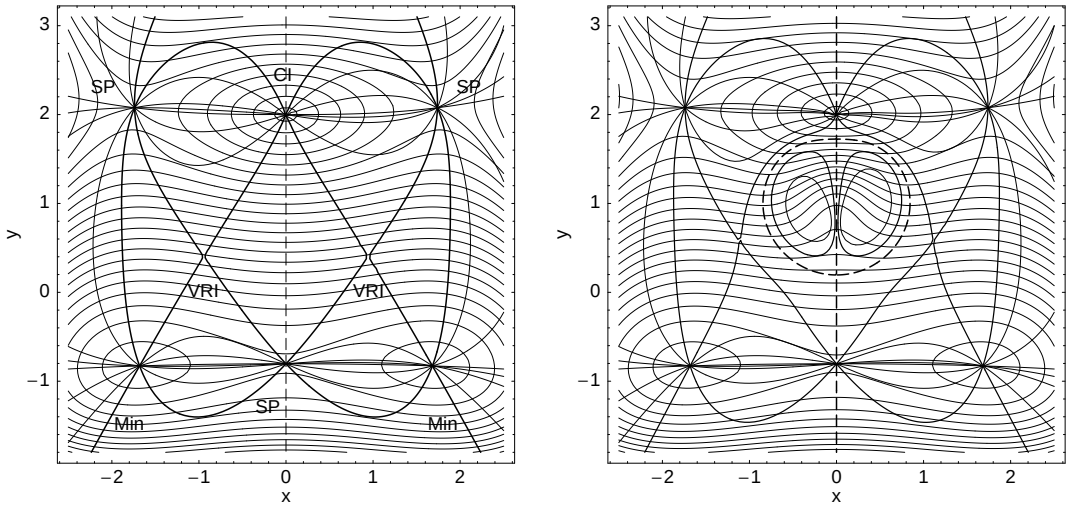


Figure 5: NTs connect stationary points. **Left:** A ridge to a CI point at (0,2). Two singular NTs connect the two minimums with the CI point which plays the role of a summit. **Right:** Compact NTs emerge inside the dent of a thumb on the ridge. A further singular NT emerges with two VRIs on the y-axis (bold dashes).